

# SUSY effects in Higgs productions at high energy $e^+e^-$ colliders

---

Junjie Cao<sup>1</sup>, Chengcheng Han<sup>2</sup>, Jie Ren<sup>1</sup>, Lei Wu<sup>3</sup>, Jin Min Yang<sup>4</sup>, Yang Zhang<sup>4</sup>

<sup>1</sup> *Physics Department, Henan Normal University, Xinxiang 453007, China*

<sup>2</sup> *Asia Pacific Center for Theoretical Physics, San 31, Hyoja-dong, Nam-gu, Pohang 790-784, Republic of Korea*

<sup>3</sup> *ARC Centre of Excellence for Particle Physics at the Terascale, School of Physics, University of Sydney, NSW 2006, Australia*

<sup>4</sup> *State Key Laboratory of Theoretical Physics, Institute of Theoretical Physics, Academia Sinica, Beijing 100190, China*

**ABSTRACT:** Considering the constraints from collider experiments and dark matter detections, we investigate the SUSY effects in the Higgs productions  $e^+e^- \rightarrow Zh$  at an  $e^+e^-$  collider with a center-of-mass energy above 240 GeV and  $\gamma\gamma \rightarrow h \rightarrow b\bar{b}$  at a photon collider with a center-of-mass energy above 125 GeV. In the parameter space allowed by current experiments, we find that the SUSY corrections to  $e^+e^- \rightarrow Zh$  can reach a few percent and the production rate of  $\gamma\gamma \rightarrow h \rightarrow b\bar{b}$  can be enhanced by a factor of 1.2 over the SM prediction. We also calculate the exotic Higgs productions  $e^+e^- \rightarrow Zh_1$  and  $e^+e^- \rightarrow A_1h$  in the next-to-minimal supersymmetric model (NMSSM) ( $h$  is the SM-like Higgs,  $h_1$  and  $A_1$  are respectively the CP-even and CP-odd singlet-dominant Higgs bosons which can be much lighter than  $h$ ). We find that at a 250 GeV  $e^+e^-$  collider the production rates of  $e^+e^- \rightarrow Zh_1$  and  $e^+e^- \rightarrow A_1h$  can reach 60 fb and 0.1 fb, respectively.

---

## Contents

<b>1</b>	<b>Introduction</b>	<b>1</b>
<b>2</b>	<b>Calculations</b>	<b>2</b>
2.1	A description of calculations	2
2.2	Calculations for $e^+e^- \rightarrow Zh$	5
2.3	Calculations for $\gamma\gamma \rightarrow h$	6
<b>3</b>	<b>Numerical results and discussions</b>	<b>7</b>
3.1	Results for $e^+e^- \rightarrow Zh$ in MSSM and CMSSM	7
3.2	Results for $\gamma\gamma \rightarrow h \rightarrow b\bar{b}$ in MSSM	8
3.3	Results for $e^+e^- \rightarrow Zh_1$ and $e^+e^- \rightarrow hA_1$ in NMSSM	9
<b>4</b>	<b>Conclusion</b>	<b>10</b>

---

## 1 Introduction

The LHC has discovered a scalar with mass around 125 GeV which resembles the Standard Model (SM) Higgs boson [1]. Since the minimal supersymmetric model (MSSM) predicts a light Higgs boson below 130 GeV [2], the discovery of such a 125 GeV Higgs boson may be the first hint of low energy supersymmetry (SUSY). However, the LHC measurements of the properties of this new boson are so far consistent with the SM predictions, which squeezes the SUSY effects in the Higgs couplings to a decoupling region [3–5]. Besides, after the LHC Run-1, the null results of direct searches for SUSY particles (sparticles) have excluded the first two generation squarks and gluino with mass below about 1 TeV [6]. The third generation squarks and non-colored sparticles as light as hundreds of GeV are still allowed but have also been constrained by the LHC searches [7]. All these indicate that the SUSY scale may be much higher than the electroweak scale. So it will be a challenge for the LHC to directly observe any SUSY particles except for the alone light Higgs boson. In such a situation, an alternative way for probing SUSY is to search for the indirect SUSY loop effects from some precision measurements of the Higgs boson. Since the precision measurements of the Higgs boson are rather challenging at hadron colliders like the LHC, some high energy  $e^+e^-$  colliders with center-of-mass energy above 240 GeV are being proposed.

At an  $e^+e^-$  collider, the Higgs-strahlung process  $e^+e^- \rightarrow Zh$  is the dominant production channel for the Higgs boson, for which the  $Zh$  events can be inclusively detected by tagging a leptonic  $Z$  decay without assuming the Higgs decay mode. For a center-of-mass energy of 240 – 250 GeV and an integrated luminosity of  $500 \text{ fb}^{-1}$ , an  $e^+e^-$  collider can produce about  $O(10^5)$  Higgs bosons per year and allow for measuring the Higgs couplings

at percent level [8, 9], which may be able to unravel the SUSY effects in this production. For this process, the leading order rate, the one-loop electroweak corrections and the SUSY corrections were calculated in [10], [11–14] and [15], respectively.

As a feasible option, the  $\gamma\gamma$  collision can be achieved through the backward Compton scattering of laser light against high-energy electrons at a linear  $e^+e^-$  collider. At such a  $\gamma\gamma$  collision the Higgs boson can be singly produced via the loop process  $\gamma\gamma \rightarrow h$ . This process is demonstrated to be sensitive to the new charged SUSY particles. So the photon collider will be an ideal place to investigate the anomalous  $h\gamma\gamma$  coupling. At the  $\gamma\gamma$  collider, the Higgs partial width  $\Gamma_{\gamma\gamma}$  can be measured with an accuracy of about 2%. Besides, the  $CP$  property of the Higgs boson can be measured using the photon polarizations. The single production of SUSY Higgs bosons through  $\gamma\gamma$  fusion has been calculated in [16, 17].

Note that at a high energy  $e^+e^-$  collider the productions of some exotic Higgs bosons will be possible. If the center-of-mass energy is designed at 240-250 GeV, the production  $e^+e^- \rightarrow hA$  in the MSSM, which is complementary to the production  $e^+e^- \rightarrow Zh$  and was searched at LEP2, will not be open because the CP-odd Higgs  $A$  is now much heavier than the SM-like Higgs  $h$ . However, in the NMSSM the lightest CP-even Higgs  $h_1$  and CP-odd Higgs  $A_1$  can be singlet-dominant and much lighter than the SM-like Higgs  $h$  [18]. So in the NMSSM the exotic Higgs productions  $e^+e^- \rightarrow Zh_1$  and  $e^+e^- \rightarrow hA_1$  may occur at a 240-250 GeV  $e^+e^-$  collider. These exotic Higgs productions could be a good probe for non-minimal SUSY like the NMSSM.

In this work we examine systematically all the above processes in SUSY. We will not only calculate the NMSSM processes  $e^+e^- \rightarrow Zh_1$  and  $e^+e^- \rightarrow hA_1$  which have not been intensively studied in the literature, but also re-examine the SUSY effects in  $e^+e^- \rightarrow Zh$  and  $\gamma\gamma \rightarrow h$  by considering current experimental constraints, such as the LHC Higgs data and the dark matter detection limits.

This work is organized as follows. In Sec. II we describe the parameter scan and the calculation details for the processes  $e^+e^- \rightarrow Zh$ ,  $\gamma\gamma \rightarrow h \rightarrow b\bar{b}$ ,  $e^+e^- \rightarrow Zh_1$  and  $e^+e^- \rightarrow A_1h$ . In Sec.III, we show the numerical results. Finally, we draw the conclusions in Sec. IV.

## 2 Calculations

### 2.1 A description of calculations

There are about 120 free parameters in a general  $R$ -parity conserving weak-scale MSSM. However, most of these parameters are related to the flavor changing neutral currents (FCNC) and/or the  $CP$ -violating phases, which are highly constrained by the experimental measurements. So in our work we only discuss the pMSSM and CMSSM, where the free parameters are reduced and the models are more predictive.

The pMSSM is considered as the most general version of the  $R$ -parity conserving MSSM with the following considerations

- (i)  $CP$  conservation;
- (ii) The principle of minimal flavor violation (MFV) at the weak scale;

- (iii) Degenerate masses of the first and second generation sfermions;
- (iv) Negligible Yukawa couplings and trilinear terms for the first two generations, but keeping the 3rd generation parameters  $A_t, A_b, A_\tau$ ;
- (v) The lightest neutralino as the LSP.

Finally, only 19 parameters can be independently changed in the pMSSM, which are

- (a)  $\tan\beta$ , which is the ratio of the vevs of the two Higgs doublet fields;
- (b) the higgsino mass parameter  $\mu$  and the pseudo-scalar Higgs mass  $m_A$ ;
- (c) the gaugino mass parameters  $M_1, M_2, M_3$  ;
- (d) the first/second generation sfermion mass parameters  $m_{\tilde{q}}, m_{\tilde{u}_R}, m_{\tilde{d}_R}, m_{\tilde{l}}, m_{\tilde{e}_R}$ ;
- (e) the third generation sfermion mass parameters  $m_{\tilde{Q}}, m_{\tilde{t}_R}, m_{\tilde{b}_R}, m_{\tilde{L}}, m_{\tilde{\tau}_R}$ ;
- (f) the third generation trilinear couplings  $A_t, A_b, A_\tau$ .

To further simplify the parameter space we assume  $M_1 : M_2 = 1 : 2$ ,  $A_t = A_b = A_\tau = A_e$  and  $m_{t_R} = m_{b_R}, m_{\tau_R} = m_{e_R}, m_l = m_L$ . We also take a common mass  $M_{SUSY} = m_q = m_{u_R} = m_{d_R} = M_3 = 2$  TeV to avoid the constraints from the first-two generation squarks and the gluino direct searches at the LHC. In addition, considering the current bounds on the stop and stau masses in the MSSM, we conservatively require the lighter stop mass  $m_{\tilde{t}_1} > 300$  GeV and the lighter stau mass  $m_{\tilde{\tau}} > 150$  GeV. We scan the parameters space in the following ranges

$$\begin{aligned}
|A_t| &\leq 5 \text{ TeV}, & 100 \text{ GeV} &\leq (M_{\tilde{Q}}, M_{t_R}) \leq 3 \text{ TeV}, \\
1 &\leq \tan\beta \leq 50, & 90 \text{ GeV} &\leq M_A \leq 1.5 \text{ TeV}, \\
100 \text{ GeV} &\leq \mu \leq 1 \text{ TeV}, & 100 \text{ GeV} &\leq (M_L, M_l, M_2) \leq 3 \text{ TeV}.
\end{aligned} \tag{2.1}$$

Different from the general MSSM where all soft breaking parameters are independent [19], the CMSSM [20] assumes the following universal soft breaking parameters at SUSY breaking scale (usually chosen as the Grand Unification scale) as the fundamental ones:

$$M_{1/2}, M_0, A_0, \tan\beta, \text{sign}(\mu), \tag{2.2}$$

with  $M_{1/2}$ ,  $M_0$  and  $A_0$  denoting the gaugino mass, scalar mass and trilinear interaction coefficient, respectively. When evolving these parameters down to weak scale, we get all the soft breaking parameters in the low energy MSSM. The ranges of these parameters in our scan are

$$\begin{aligned}
200 \text{ GeV} &\leq m_0 \leq 4 \text{ TeV}, \\
200 \text{ GeV} &\leq m_{1/2} \leq 4 \text{ TeV}, \\
-4 \text{ TeV} &\leq A_0 \leq 4 \text{ TeV}, \\
2 &\leq \tan\beta \leq 65.
\end{aligned} \tag{2.3}$$

For the NMSSM, we scan the parameters in the following ranges

$$\begin{aligned}
|A_t| &\leq 3 \text{ TeV}, & 100 \text{ GeV} &\leq (M_Q, M_{t_R}) \leq 2 \text{ TeV}, \\
1 &\leq \tan\beta \leq 10, & 90 \text{ GeV} &\leq M_A \leq 1 \text{ TeV}, \\
100 \text{ GeV} &\leq \mu \leq 300 \text{ TeV}, & 100 \text{ GeV} &\leq (M_L, M_l, M_2) \leq 3 \text{ TeV}. \\
0.001 &\leq \lambda \leq 0.8, & 0.001 &\leq \kappa \leq 0.8, & -300 \text{ GeV} &\leq A_\kappa \leq 300 \text{ GeV}
\end{aligned} \tag{2.4}$$

and other parameters like first/second generation squark mass and gluino mass are set to be 2 TeV.

In our scan, we impose the following constraints

- (1) A SM-like Higgs mass in the range of 123-127 GeV. We use FeynHiggs-2.8.9 [21] to calculate the Higgs mass and impose the experimental constraints from LEP, Tevatron and LHC with HiggsBounds-3.8.0 [22]. We do not perform the Higgs couplings fit to the LHC data because of the current poor precisions.
- (2) Various  $B$ -physics bounds at  $2\sigma$  level. We implement the constraints by using the package of SuperIso v3.3 [23], including  $B \rightarrow X_s \gamma$  and the latest measurements of  $B_s \rightarrow \mu^+ \mu^-$ ,  $B_d \rightarrow X_s \mu^+ \mu^-$  and  $B^+ \rightarrow \tau^+ \nu$ .
- (3) The thermal relic density of the lightest neutralino is in the  $2\sigma$  range of the Planck data [24] and the dark matter  $\sigma^{SI}$  upper limit from the LUX data [25]. The code MicrOmega v2.4 [26] are used to calculate the relic density.
- (4) The constraints from the electroweak observables such as  $\rho_t$ ,  $\sin^2 \theta_{eff}^l$ ,  $m_W$  and  $R_b$  [27] at  $2\sigma$  level.
- (5) We require the MSSM and NMSSM to explain at  $2\sigma$  level the discrepancy of the measured value of the muon anomalous magnetic moment from its SM prediction, i.e.,  $a_\mu^{exp} - a_\mu^{SM} = (28.7 \pm 8.0) \times 10^{-10}$  [28]. While for the CMSSM, since there is a tension between  $\mu_{g-2}$  with the Higgs mass [29], we just require the CMSSM prediction not worse than the SM value.
- (6) Since the large mixing terms in the stop/stau sector will affect the vacuum stability, we require SUSY to comply with the vacuum meta-stability condition by using the formulas in [30, 31].

We also impose the multi-jets direct search limits [32] on the  $(m_0, m_{1/2})$  plane based on the search by the ATLAS collaboration for squarks and gluinos in the final states that contain missing  $E_T$ , jets and 0 – 1 leptons in  $20.1 - 20.7 \text{ fb}^{-1}$  integrated luminosity of data at  $\sqrt{s} = 8 \text{ TeV}$  collision energy. While these exclusion limits were obtained in the MSUGRA/CMSSM framework for fixed value of  $\tan\beta$  and  $A_0 = -2m_0$ , it was proved [33] that the result is fairly insensitive to  $\tan\beta$  and  $A_0$  and so we can use the limits directly.

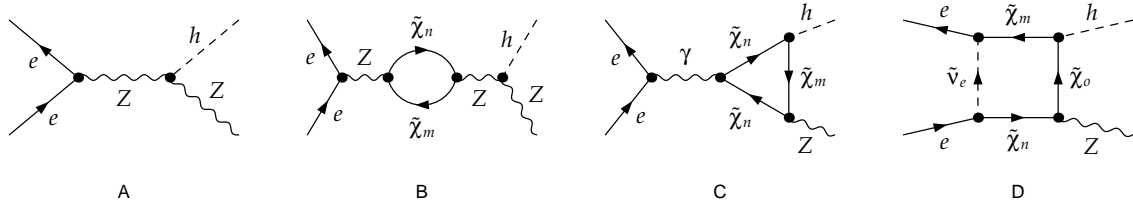


**Figure 1.** The representative Feynman diagrams for  $e^+e^- \rightarrow Zh$  in the MSSM: (A) is the tree level diagram, and (B-D) are the self-energy, triangle and box diagrams, respectively.

Besides, to make the SM-like Higgs not deviate from the Higgs data largely, we also impose following constraints on the property of the SM-like Higgs

$$0.8 \leq \frac{\sigma(pp \rightarrow h) \times Br(h \rightarrow \gamma\gamma)}{(\sigma \times Br)_{SM}} \leq 1.5 \quad (2.5)$$

$$0.8 \leq \frac{\sigma(pp \rightarrow h) \times Br(h \rightarrow WW/ZZ)}{(\sigma \times Br)_{SM}} \leq 1.2 \quad (2.6)$$

In the calculations, we generate and simplify the amplitudes by using the packages `FeynArts-3.9` [34] and `FormCalc-8.2`[35]. All the loop functions are numerically calculated with the package `LoopTools-2.8` [36].

## 2.2 Calculations for $e^+e^- \rightarrow Zh$

The one-loop corrections for  $e^+e^- \rightarrow Zh$  in the SM and MSSM have been studied in [2]. In Fig. 1 we show the typical Feynman diagrams for the  $e^+e^- \rightarrow Zh$  production in the MSSM.

The complete one-loop corrections to the process  $e^+e^- \rightarrow Zh$  include two parts: virtual corrections and real photon radiations. The virtual corrections include a set of self-energy corrections, the vertex corrections of  $eeZ$ ,  $ZZh$  and  $ZAh$ , and the box diagrams. We adopt the dimensional regularization and the constrained differential renormalization (CDR) [37] to regulate the ultraviolet divergence (UV) in the loop amplitudes for the SM and MSSM, respectively. These UV singularities are removed by using the on-shell renormalization scheme. We take the definitions of the scalar and tensor two-, three- and four-integral functions presented in [38] and use Passarino-Veltman method to reduce the  $N$ -point tensor functions to scalar integrals [39].

Due to the infrared (IR) singularities in the vertex corrections to  $e^+e^- \rightarrow Zh$ , the real photon radiation corrections should be taken into account. These IR divergences can be canceled with the real photon bremsstrahlung corrections in the soft photon limit by the Kinoshita-Lee-Nauenberg theorem [40]. According to the energy of the photon  $E_\gamma$ , we split the phase space into a soft region ( $E_\gamma < \Delta E_\gamma \ll \sqrt{s}/2$ ) and a hard region ( $E_\gamma > \Delta E_\gamma \gg \sqrt{s}/2$ ), where  $\Delta E_\gamma$  is the energy cut-off of the soft photon. We use the soft photon approximation formula to obtain the soft part of the cross section [41] and give a fictitious mass  $m_\gamma$  to the photon to eliminate the IR divergence. It should be noted that the dependence of the real corrections on  $m_\gamma$  is exactly canceled by the corresponding virtual

corrections. In the hard region, we use the well-known VEGAS [42] routine to evaluate the cross section. We checked that our results are independent of  $m_\gamma$  and  $\Delta E_\gamma$ .

### 2.3 Calculations for $\gamma\gamma \rightarrow h$

The leading order  $\gamma\gamma \rightarrow h$  occurs at one-loop level, where the photon beam is generated by the backward Compton scattering of the incident electron- and the laser-beam. The number of events is obtained by convoluting the cross section of  $\gamma\gamma$  collision with the photon beam luminosity distribution given by

$$N_{\gamma\gamma \rightarrow h} = \int d\sqrt{s_{\gamma\gamma}} \frac{d\mathcal{L}_{\gamma\gamma}}{d\sqrt{s_{\gamma\gamma}}} \hat{\sigma}_{\gamma\gamma \rightarrow h}(s_{\gamma\gamma}) \equiv \mathcal{L}_{e^+e^-} \sigma_{\gamma\gamma \rightarrow h}(s) \quad (2.7)$$

where  $d\mathcal{L}_{\gamma\gamma}/d\sqrt{s_{\gamma\gamma}}$  is the photon-beam luminosity distribution and  $\sigma_{\gamma\gamma \rightarrow h}(s)$  ( $s$  is the squared center-of-mass energy of  $e^+e^-$  collision) is defined as the effective cross section of  $\gamma\gamma \rightarrow h$ . In the optimal case, it can be written as [43]

$$\sigma_{\gamma\gamma \rightarrow h}(s) = \int_{\sqrt{a}}^{x_{max}} 2z dz \hat{\sigma}_{\gamma\gamma \rightarrow h}(s_{\gamma\gamma} = z^2 s) \int_{z^2/x_{max}}^{x_{max}} \frac{dx}{x} F_{\gamma/e}(x) F_{\gamma/e}\left(\frac{z^2}{x}\right) \quad (2.8)$$

where  $F_{\gamma/e}$  denotes the energy spectrum of the back-scattered photon for the unpolarized initial electron and laser photon beams given by

$$F_{\gamma/e}(x) = \frac{1}{D(\xi)} \left[ 1 - x + \frac{1}{1-x} - \frac{4x}{\xi(1-x)} + \frac{4x^2}{\xi^2(1-x)^2} \right] \quad (2.9)$$

with

$$D(\xi) = \left(1 - \frac{4}{\xi} - \frac{8}{\xi^2}\right) \ln(1 + \xi) + \frac{1}{2} + \frac{8}{\xi} - \frac{1}{2(1 + \xi)^2}. \quad (2.10)$$

Here  $\xi = 4E_e E_0/m_e^2$  ( $E_e$  is the incident electron energy and  $E_0$  is the initial laser photon energy) and  $x = E/E_0$  with  $E$  being the energy of the scattered photon moving along the initial electron direction.

In the calculations of  $e^+e^- \rightarrow Zh$  and  $\gamma\gamma \rightarrow h \rightarrow b\bar{b}$ , we use the package FeynHiggs to obtain the masses of the Higgs bosons in the MSSM. By evaluating loop corrections to the  $h$ ,  $H$  and  $hH$ -mixing propagators, we can determine the masses of the two  $CP$ -even Higgs bosons  $m_h$  and  $m_H$  as the poles of this propagator matrix, which are given by the solution of

$$[q^2 - m_h^{2,tree} + \hat{\Sigma}_{hh}(q^2)][q^2 - m_H^{2,tree} + \hat{\Sigma}_{HH}(q^2)] - [\hat{\Sigma}_{hH}(q^2)]^2 = 0 \quad (2.11)$$

where  $\hat{\Sigma}_{hH}(q^2)$ ,  $\hat{\Sigma}_{HH}(q^2)$  and  $\hat{\Sigma}_{hh}(q^2)$  denote the renormalized Higgs boson self-energies. It should be noted that since the Higgs field renormalization constants are given in the  $\overline{DR}$  scheme [44] in FeynArts-3.9, we adopt the finite wave function normalization factors  $\hat{Z}_{ij}$  to ensure the correct on-shell properties of the external particles in the  $S$ -matrix elements. The values of  $\hat{Z}_{ij}$  can be numerically obtained by using the package FeynHiggs.

Also, it should be noted that normally one has to use the tree-level Higgs masses in the whole loop calculations to keep the gauge invariance, while for the phase space integration

we need to express the matrix element in terms of the physical masses for the external final-states. In our study, we take the loop-corrected Higgs boson mass as the physical mass and adopt the proposed way in [45] to technically deal with this problem. To be specific, since the tree-level process  $e^+e^- \rightarrow Zh$  does not involve the exchange of the light Higgs boson  $h$ , we only need to use tree-level Higgs masses in the loop integral calculation but keep the loop-corrected mass in the phase space integration.

### 3 Numerical results and discussions

The SM input parameters are taken as [46]

$$\begin{aligned} m_t &= 172.00 \text{ GeV}, \quad m_Z = 91.1876 \text{ GeV}, \\ \alpha(m_Z) &= 1/127.9, \quad \sin^2 \theta_W = 0.231, \quad \alpha_s(m_Z) = 0.1185. \end{aligned} \quad (3.1)$$

We define the following ratio to quantitatively show the SUSY effect in the Higgs productions

$$\frac{\Delta\sigma^{SUSY}}{\sigma_{SM}} = \frac{\sigma^{SUSY} - \sigma^{SM}}{\sigma^{SM}} \quad (3.2)$$

where  $\sigma^{SUSY}$  and  $\sigma^{SM}$  are the one-loop cross sections in the MSSM and SM, respectively.

#### 3.1 Results for $e^+e^- \rightarrow Zh$ in MSSM and CMSSM

In Fig.2 we show the dependence of SUSY corrections to the process  $e^+e^- \rightarrow Zh$  on the chargino mass  $m_{\tilde{\chi}_1^+}$  for the samples allowed by constraints (1)-(6) at  $2\sigma$  level for an  $e^+e^-$  collider with  $\sqrt{s} = 250, 350, 500$  GeV. From this figure we can see that the SUSY corrections can be negative or positive, depending on the masses of the sparticles in the loops and the collider energies. For  $\sqrt{s} = 250$  GeV, the SUSY corrections can maximally reach  $-2.5\%$  with  $m_{\tilde{\chi}_1^+} \sim \sqrt{s}/2$ , which is caused by the resonant effects in the chargino loops. Note that the bounds on the chargino mass from direct electroweakinos searches are still weak for our samples since most of the survived points are dominated by the mixture of wino-higgsino. Given the expected sensitivity of a 250 GeV  $e^+e^-$  collider like CEPC, the residual SUSY effects in  $e^+e^- \rightarrow Zh$  can still be detected if  $m_{\tilde{\chi}_1^+} < 400$  GeV when the luminosity reach about  $10,000 \text{ fb}^{-1}$  [47]. Since the  $hZZ$  coupling directly affects the  $Zh$  production, we survey the deviation of this coupling from the SM value and find it at most 0.05%. So in the MSSM the difference of  $Zh$  production from the SM is largely from the sparticle contribution.

In Fig.3 we present the dependence of SUSY corrections to the process  $e^+e^- \rightarrow Zh$  on the neutralino mass  $m_{\tilde{\chi}_1^0}$  in the CMSSM with  $\sqrt{s} = 250, 350, 500$  GeV. We find that the SUSY corrections for almost samples are less than 0.5% because the sparticles masses have been pushed up to multi-hundreds GeV region by the inclusive sparticles searches for the CMSSM at the LHC. So it is difficult to observe these indirect CMSSM loop effects through  $e^+e^- \rightarrow Zh$  production at future  $e^+e^-$  colliders.



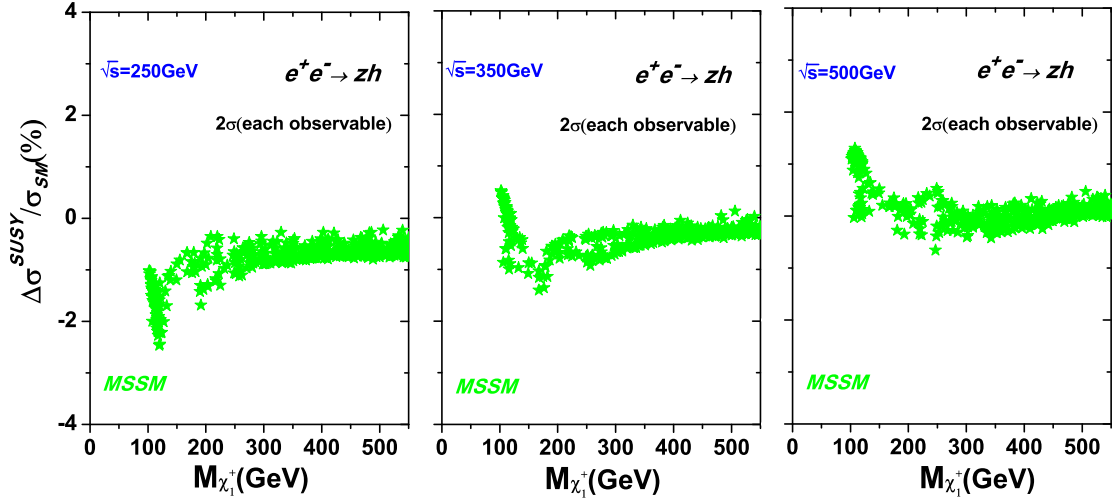


**Figure 2.** The MSSM corrections to the process  $e^+e^- \rightarrow Zh$  for the samples allowed by constraints (1)-(6) at  $2\sigma$  level for an  $e^+e^-$  collider with  $\sqrt{s} = 250, 350, 500$  GeV.

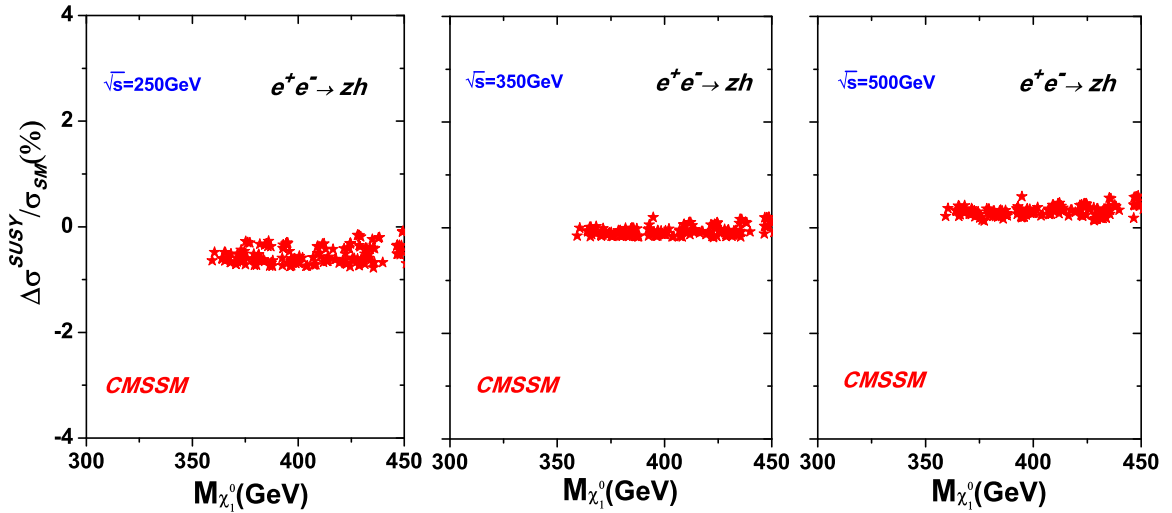


**Figure 3.** Same as Fig.2, but for the CMSSM.

### 3.2 Results for $\gamma\gamma \rightarrow h \rightarrow b\bar{b}$ in MSSM

At an ILC-based photon collider, the Higgs boson can be singly produced through the photon-photon fusion mechanism. Since the cross section of  $\gamma\gamma \rightarrow h$  is proportional to the decay width of  $h \rightarrow \gamma\gamma$ , the ratio  $\Delta\sigma^{SUSY}(\gamma\gamma \rightarrow h)/\sigma^{SM}(\gamma\gamma \rightarrow h)$  is independent of the energy of ILC. Given the large branching ratio of  $h \rightarrow b\bar{b}$ , we calculate the SUSY corrections to the observable  $\sigma(\gamma\gamma \rightarrow h) \cdot Br(h \rightarrow b\bar{b})$  in the MSSM and display its dependence on the mass of pseudo-scalar  $m_A$  in Fig.4.

From Fig.4 we can see that the SUSY corrections can maximally reach 20% for the allowed samples in the small  $m_A$  region with a large  $\tan\beta$  due to the enhancement of

$Br(h \rightarrow b\bar{b})$ . With the increase of  $m_A$ , the SUSY corrections drop. Note that a light stau can make sizable loop contribution to  $\gamma\gamma \rightarrow h$ , which, after considering the vacuum stability, can enhance the cross section by a factor of 1.2.

So, if the photon-photon collision can be realized at the ILC, it will be a good place for probing SUSY effects. Of course, it should be mentioned that such sizable effects may be detected or further constrained at the LHC Run-2.

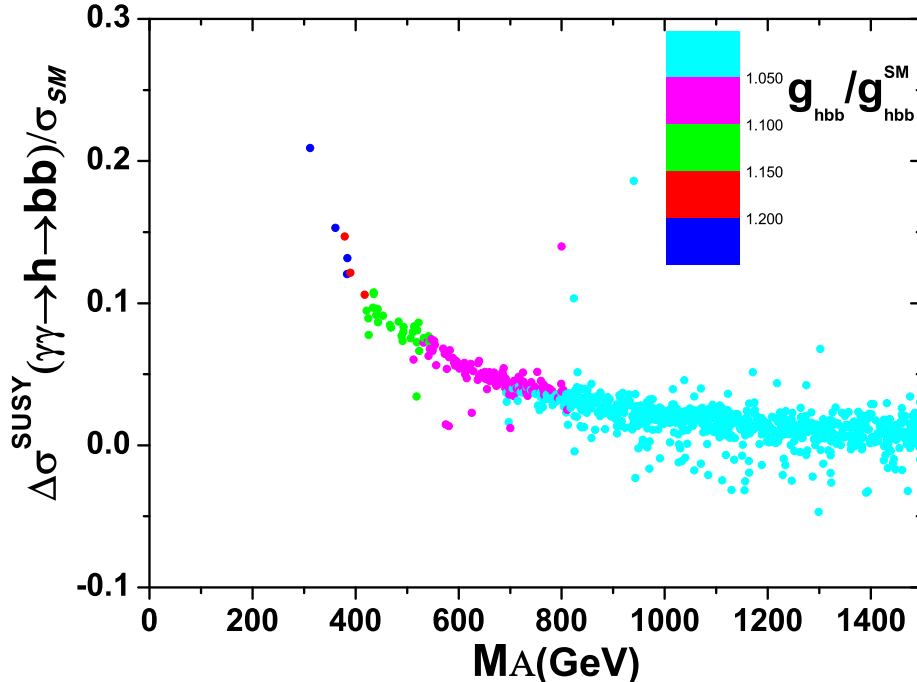


**Figure 4.** The SUSY corrections to  $\gamma\gamma \rightarrow h \rightarrow b\bar{b}$  at a photon collider with center-of-mass energy above 125 GeV.

### 3.3 Results for $e^+e^- \rightarrow Zh_1$ and $e^+e^- \rightarrow hA_1$ in NMSSM

In our scan of the NMSSM parameter space we choose  $h_2$  as the SM-like Higgs  $h$ . In this case the lightest CP-even Higgs  $h_1$  and CP-odd Higgs  $A_1$  are singlet-dominant and can be much lighter than  $h$ .

In Fig.5 we show the leading-order cross sections for  $e^+e^- \rightarrow Zh_1$  and  $e^+e^- \rightarrow A_1h$  in the NMSSM for  $\sqrt{s} = 250$  GeV. From the right panel we see that the  $e^+e^- \rightarrow Zh_1$  production rate varies between a rather large range and most samples give a cross section larger than 1 fb. It is interesting that the largest production rate increases with the mass of  $h_1$ . The reason is that the  $e^+e^- \rightarrow Zh_1$  production rate largely depends on the  $h_1ZZ$  coupling, which comes from the mixing between the singlet and the doublet Higgs fields. When the two masses of  $h_1$  and  $h$  get closer, the mixing generally become larger and thus  $e^+e^- \rightarrow Zh_1$  increases with the  $h_1$  mass. This situation is different from the  $e^+e^- \rightarrow A_1h$

production, whose cross section decreases with the increase of  $A_1$  mass since the production rate would be kinematic enhanced when  $A_1$  is light.

Note that the  $e^+e^- \rightarrow A_1h$  production rate is much smaller than  $e^+e^- \rightarrow Zh_1$ . The largest cross section can only reach 0.1 fb. The reason is that this production rate depends on the  $ZA_1h$  coupling. This couplings arises from the mixing between the two CP-odd scalars and a moderately large  $M_{A_1}$  would induce a small mixing.

The right panel of Fig.5 shows the leading-order cross sections of three production channels versus the  $hZZ$  coupling normalized to the SM value. We see that the cross section of  $e^+e^- \rightarrow Zh_1$  is sensitive to the deviation of  $hZZ$  coupling from the SM value. When the  $hZZ$  coupling approaches to the SM value, the cross section of  $e^+e^- \rightarrow Zh_1$  drops sharply. For the channel  $e^+e^- \rightarrow A_1h$ , although its production rate is much smaller than  $e^+e^- \rightarrow Zh_1$ , it is not so sensitive to the  $hVV$  coupling. We numerically checked that as the  $hZZ$  coupling approaches to the SM value, the production rate of  $e^+e^- \rightarrow A_1h$  can still reach 0.1 fb.

Since the dominant decay mode of the light Higgs bosons is  $b\bar{b}$ , the exotic Higgs productions  $e^+e^- \rightarrow A_1h$  and  $e^+e^- \rightarrow Zh_1$  will lead to  $4b$  and  $Z + 2b$ , respectively. These signals can be efficiently detected at an  $e^+e^-$  collider. Also note that at such an  $e^+e^-$  collider the loop-induced Higgs production  $e^+e^- \rightarrow h\gamma$  can get enhanced in SUSY [50]. All these processes can jointly serve as a good probe for SUSY models.

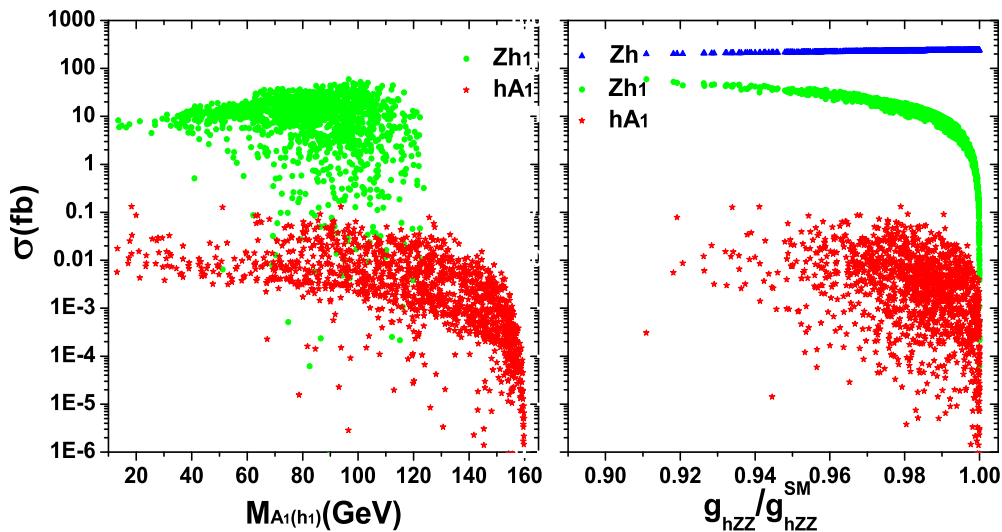


**Figure 5.** The cross sections of  $e^+e^- \rightarrow Zh_1$  and  $e^+e^- \rightarrow A_1h$  in the NMSSM for a 250 GeV  $e^+e^-$  collider.

## 4 Conclusion

In this work we examined the SUSY residual effects in the process  $e^+e^- \rightarrow Zh$  at an  $e^+e^-$  collider with center-of-mass energy above 250 GeV and  $\gamma\gamma \rightarrow h \rightarrow b\bar{b}$  at a photon

collider with center-of-mass energy above 125 GeV. We found that the SUSY corrections to  $e^+e^- \rightarrow Zh$  can reach a few percent in the parameter space allowed by current experiments. The production rate of  $\gamma\gamma \rightarrow h \rightarrow b\bar{b}$  can be enhanced by a factor of 1.2 over the SM prediction. We also calculated the exotic Higgs productions  $e^+e^- \rightarrow Zh_1$  and  $e^+e^- \rightarrow A_1h$  in the NMSSM. We found that for an  $e^+e^-$  collider with center-of-mass energy of 250 GeV the  $e^+e^- \rightarrow Zh_1$  and  $e^+e^- \rightarrow A_1h$  production rates can reach 60 fb and 0.1 fb, respectively. These processes will jointly serve as a probe of SUSY in the proposed  $e^+e^-$  collider like CEPC, TLEP or ILC.

## Acknowledgement

This work was supported by the National Natural Science Foundation of China (NNSFC) under grant Nos. 10821504, 11222548, 11305049 and 11135003, by Program for New Century Excellent Talents in University, and also by the ARC Center of Excellence for Particle Physics at the Tera-scale.

## References

- [1] G. Aad *et al.* [ATLAS Collaboration], Phys. Lett. B **716**, 1 (2012); S. Chatrchyan *et al.* [CMS Collaboration], Phys. Lett. B **716**, 30 (2012).
- [2] J. Ellis, G. Ridolfi and F. Zwirner, Phys. Lett. 262B (1991) 477; R. Barbieri and M. Frigeni, Phys. Lett. 258B (1991) 395; A. Brignole *et al.*, Phys. Lett. 271B (1991) 123; M. Carena, K. Sasaki and C.E.M. Wagner, Nucl. Phys. 381B (1992) 66; H.E. Haber, R. Hempfling, Phys. Rev. D48 (1993) 4280; P.H. Chankowski, S. Pokorski and J. Rosiek, Phys. Lett. 281B (1992) 100.
- [3] J. Cao *et al.*, JHEP **1210**, 079 (2012) [arXiv:1207.3698 [hep-ph]]; JHEP **1203**, 086 (2012) [arXiv:1202.5821 [hep-ph]]; M. Carena *et al.*, JHEP **1203**, 014 (2012); J. Ellis and K. A. Olive, Eur. Phys. J. C **72**, 2005 (2012);
- [4] G. Belanger *et al.*, Phys. Rev. D **88**, 075008 (2013).
- [5] P. P. Giardino *et al.*, arXiv:1303.3570 [hep-ph].
- [6] S. S. AbdusSalam, Phys. Rev. D **87** (2013) 115012; S. S. AbdusSalam and D. Choudhury, arXiv:1210.3331 [hep-ph].
- [7] For stop and electroweak gaugino bounds, see, e.g., C. Han *et al.*, JHEP **1310** (2013) 216 [arXiv:1308.5307 [hep-ph]]; JHEP **1402** (2014) 049 [arXiv:1310.4274 [hep-ph]]; arXiv:1409.4533 [hep-ph]; arXiv:1409.7000 [hep-ph]; J. Cao *et al.*, JHEP **1211** (2012) 039 [arXiv:1206.3865 [hep-ph]]; T. A. W. Martin and D. Morrissey, arXiv:1409.6322 [hep-ph]; L. Calibbi, J. M. Lindert, T. Ota and Y. Takanishi, arXiv:1405.3884 [hep-ph]; H. Baer, A. Mustafayev and X. Tata, Phys. Rev. D **89**, 055007 (2014) [arXiv:1401.1162 [hep-ph]]; M. Low and L. T. Wang, JHEP **1408**, 161 (2014) [arXiv:1404.0682 [hep-ph]].
- [8] M. E. Peskin, arXiv:1207.2516 [hep-ph].
- [9] A. Blondel *et al.*, arXiv:1302.3318 [physics.acc-ph]; R. Belusevic and T. Higo, arXiv:1208.4956 [physics.acc-ph].
- [10] J. R. Ellis, M. K. Gaillard and D. V. Nanopoulos, Nucl. Phys. B **106** (1976) 292;

- [11] J. Fleischer and F. Jegerlehner, Nucl. Phys. B **216**, 469 (1983); G. J. Gounaris and F. M. Renard, arXiv:1409.2596 [hep-ph].
- [12] B. A. Kniehl, Z. Phys. C **55**, 605 (1992).
- [13] A. Denner, *et al.*, Z. Phys. C **56** (1992) 261; N. Liu, *et al.*, JHEP **1404**, 189 (2014) [arXiv:1311.6971 [hep-ph]].
- [14] F. A. Berends and R. Kleiss, Nucl. Phys. B **260** (1985) 32.
- [15] P. H. Chankowski, S. Pokorski and J. Rosiek, Nucl. Phys. B **423** (1994) 437 [hep-ph/9303309]; V. Driesen and W. Hollik, Z. Phys. C **68** (1995) 485 [hep-ph/9504335]; V. Driesen, W. Hollik and J. Rosiek, Z. Phys. C **71** (1996) 259 [hep-ph/9512441].
- [16] D. Lopez-Val and J. Sola, Phys. Lett. B **702**, 246 (2011) [arXiv:1106.3226 [hep-ph]]; P. Niezurawski, A. F. Zarnecki and M. Krawczyk, eConf C **050318**, 0112 (2005) [hep-ph/0507006]; M. M. Muhlleitner *et al.*, Phys. Lett. B **508**, 311 (2001) [hep-ph/0101083].
- [17] S. Bae, B. Chung and P. Ko, Eur. Phys. J. C **54**, 601 (2008) [hep-ph/0205212]; S. Y. Choi and J. S. Lee, Phys. Rev. D **62**, 036005 (2000) [hep-ph/9912330].
- [18] J. Cao *et al.*, JHEP **1311**, 018 (2013) [arXiv:1309.4939 [hep-ph]]; N. E. Bomark, S. Moretti, S. Munir and L. Roszkowski, arXiv:1409.8393 [hep-ph].
- [19] S. Dimopoulos and D. W. Sutter, Nucl. Phys. B **452** (1995) 496 [hep-ph/9504415]; H. E. Haber, Nucl. Phys. Proc. Suppl. **62** (1998) 469 [hep-ph/9709450]; G. L. Kane, PoS silafae **-III** (2000) 013 [hep-ph/0008190];
- [20] A. H. Chamseddine, R. L. Arnowitt and P. Nath, Phys. Rev. Lett. **49** (1982) 970.
- [21] M. Frank *et al.*, JHEP **0702**, 047 (2007); G. Degrassi *et al.*, Eur. Phys. J. C **28**, 133 (2003); S. Heinemeyer, W. Hollik and G. Weiglein, Comput. Phys. Commun. **124**, 76 (2000); Eur. Phys. J. C **9**, 343 (1999).
- [22] P. Bechtle *et al.*, Comput. Phys. Commun. **182**, 2605 (2011); Comput. Phys. Commun. **181**, 138 (2010).
- [23] F. Mahmoudi, Comput. Phys. Commun. **180**, 1579 (2009); Comput. Phys. Commun. **178**, 745 (2008).
- [24] P. A. R. Ade *et al.* [Planck Collaboration], arXiv:1303.5076 [astro-ph.CO].
- [25] D. S. Akerib *et al.* [LUX Collaboration], Phys. Rev. Lett. **112** (2014) 091303 [arXiv:1310.8214 [astro-ph.CO]].
- [26] G. Belanger *et al.*, Comput. Phys. Commun. **182**, 842 (2011).
- [27] J. Cao and J. M. Yang, JHEP **0812**, 006 (2008).
- [28] J. Beringer *et al.* [Particle Data Group Collaboration], Phys. Rev. D **86** (2012) 010001.
- [29] J. Cao *et al.*, Phys. Lett. B **710**, 665 (2012) [arXiv:1112.4391 [hep-ph]].
- [30] J. -h. Park, Phys. Rev. D **83**, 055015 (2011) [arXiv:1011.4939 [hep-ph]]; D. Chowdhury *et al.*, arXiv:1310.1932 [hep-ph]; M. Bobrowski *et al.*, arXiv:1407.2814 [hep-ph].
- [31] T. Kitahara and T. Yoshinaga, arXiv:1303.0461 [hep-ph].
- [32] ATLAS collaboration,  
ATLAS-CONF-2013-047;ATLAS-CONF-2013-061;ATLAS-CONF-2013-062;  
ATLAS-CONF-2013-026;ATLAS-CONF-2013-007;arXiv:1308.1841.

- [33] B. C. Allanach, Phys. Rev. D **83**, 095019 (2011) [arXiv:1102.3149 [hep-ph]].
- [34] T. Hahn, Comput. Phys. Commun. **140** (2001) 418.
- [35] T. Hahn, M. Perez-Victoria, Comput. Phys. Commun. **118** (1999) 153.
- [36] G. J. van Oldenborgh, Phys Commun **66**, 1, NIKHEF-H-90-15 (1991); G.t Hooft and M. Veltman, Nucl. Phys. B **153**, 365 (1979); A. Denner, Fortschr. Phys. **41**, 307 (1993).
- [37] F. del Aguila, A. Culatti, R. Tapia, and M. Perez-Victoria, Nucl. Phys. B537, 561 (1999); W. Siegel, Phys. Lett. B84, 193 (1979); T. Hahn and M. Perez-Victoria, Comput. Phys. Commun. **118**, 153 (1999), hep-ph/9807565.
- [38] A. Denner, Fortschr. Phys. **41**, 307 (1993).
- [39] G.t Hooft and M. Veltman, Nucl. Phys. B153, 365 (1979); A. Denner, Fortschr. Phys. **41**, 307 (1993).
- [40] T. Kinoshita, J. Math. Phys. **3**(1962) 650; T.D. Lee and M. Nauenberg, Phys. Rev. **133**(1964) 1549.
- [41] S. Dawson and L. Reina, Phys. Rev. D59, 054012 (1999).
- [42] G.P. Legage, J. Comput. Phys. **27**, 192(1978).
- [43] I. F. Ginzburg et al., Nucl. Instrum **219**, 5 (1984); V. I. Telnov, Nucl. Instrum. Meth. **294**, 72 (1990).
- [44] M. Frank *et al.*, JHEP **0702** (2007) 047 [hep-ph/0611326]; A. Brignole, Phys. Lett. B **281** (1992) 284; M. Frank *et al.*, hep-ph/0212037; A. Freitas and D. Stockinger, hep-ph/0210372; A. Bharucha *et al.*, JHEP **1305** (2013) 053 [arXiv:1211.3134 [hep-ph]]; T. Fritzsche *et al.*, Comput. Phys. Commun. **185** (2014) 1529 [arXiv:1309.1692 [hep-ph]].
- [45] A. Freitas, A. von Manteuffel and P. M. Zerwas, Eur. Phys. J. C **40**, 435 (2005) [hep-ph/0408341].
- [46] J.Beringer et al., (Particle Data Group), Phys. Rev. D **86**, 010001 (2012).
- [47] S. Dawson *et al.*, arXiv:1310.8361 [hep-ex]; T. Han, Z. Liu and J. Sayre, arXiv:1311.7155 [hep-ph]; M. E. Peskin, arXiv:1312.4974 [hep-ph]; P. Bechtel *et al.*, arXiv:1403.1582 [hep-ph].
- [48] M. Koratzinos *et al.* arXiv:1305.6498 [physics.acc-ph]; M. Bicer *et al.* [TLEP Design Study Working Group Collaboration], JHEP **1401**, 164 (2014) [arXiv:1308.6176 [hep-ex]].
- [49] S. A. Bogacz *et al.*, arXiv:1208.2827 [physics.acc-ph]; D. M. Asner, J. B. Gronberg and J. F. Gunion, Phys. Rev. D **67** (2003) 035009 [hep-ph/0110320]; I. F. Ginzburg *et al.*, JETP Lett. **34** (1981) 491; I. F. Ginzburg *et al.*, Nucl. Instrum. Meth. **205** (1983) 47. B. Badelek *et al.*, [ECFA/DESY Photon Collider Working Group Collaboration], Int. J. Mod. Phys. A **19** (2004) 5097 [hep-ex/0108012]; P. Niezurawski, A. F. Zarnecki and M. Krawczyk, hep-ph/0307183; D. Asner *et al.*, Eur. Phys. J. C **28** (2003) 27 [hep-ex/0111056]; W. Chou *et al.*, arXiv:1305.5202 [physics.acc-ph]; V. I. Telnov, arXiv:1308.4868 [physics.acc-ph].
- [50] S. L. Hu, *et al.*, arXiv:1402.3050 [hep-ph].